Harnessing Alkali Assisted *Calotropis Gigantea* Leaf as Phytosorbent for Removal of Crystal Violet from Water

A PROJECT WORK

SUBMITTED IN THE PARTIAL FULFILLMENT OF THE REQUIREMENT FOR THE AWARD OF THE DEGREE OF MASTER OF SCIENCE

IN

CHEMISTRY

SUBMITTED BY

RACHANA
(2K23/MSCCHE/32)

Under the supervision of

Prof. ANIL KUMAR

DEPARTMENT OF APPLIED CHEMISTRY

DELHI TECHNOLOGICAL UNIVERSITY

(Formerly Delhi College of Engineering) Bawana Road, Delhi-110042

DELHI TECHNOLOGICAL UNIVERSITY

(Formerly Delhi College of Engineering Bawana Road, Delhi-110042

CANDIDATE'S DECLARTION

I, **Rachana** (Enrollment No. 2K23/MSCCHE/32), a student of M.Sc. Chemistry, hereby declare that the dissertation titled **"Harnessing Alkali-Assisted *Calotropis gigantea* Leaf as a Phytosorbent for the Removal of Crystal Violet from Water"** has been prepared and submitted by me in partial fulfillment of the requirements for the degree of Master of Science at the Department of Applied Chemistry, Delhi Technological University, Delhi. I affirm that this work is the result of my independent effort and has not been copied or reproduced from any source without appropriate citation. Furthermore, this dissertation has not been submitted previously, in whole or in part, for the award of any degree, diploma, fellowship, or any other academic recognition.

Place: Delhi

Date: 20/06/2025

Rachana

2k23/MSCCHE/32

Department of Applied Chemistry

DELHI TECHNOLOGICAL UNIVERSITY

(Formerly Delhi College of Engineering)Bawana Road, Delhi-110042

CERTIFICATE

I/We hereby certify that the Project Dissertation titled "**Harnessing Alkali Assisted *Calotropis Gigantea* Leaf as Phytosorbent for Removal of Crystal Violet from Water** " which is submitted by Rachana (2k23/MSCCHE/32), Department of Applied Chemistry, Delhi Technological University, Delhi in partial fulfillment of the requirement for the award of the Master of Science, is a record of the project work carried out bythe student under my supervision. To the best of my/our knowledge this work has not been submitted in part or full for any Degree or Diploma to this University or elsewhere.

Date: 20/06/2025

Prof. Anil Kumar

(Supervisor)

Dedicated

To

My Family

ACKNOWLEDGEMENT

It is with great pleasure and sincere gratitude that I extend my heartfelt thanks to my supervisor, **Prof. Anil Kumar (Head of Department)**, Department of Applied Chemistry, Delhi Technological University, Delhi, for his invaluable guidance and support throughout the course of this research. Despite his numerous commitments, Prof. Kumar was always generous with his time, offering thoughtful advice and constructive feedback that played a crucial role in shaping and refining the research problem. His encouragement, enthusiasm, and deep insights were instrumental in helping me navigate the challenges of this M.Sc. dissertation. I consider myself truly fortunate to have had the opportunity to learn and grow under his mentorship.

I am equally thankful to the entire faculty of the Department of Applied Chemistry for their constant encouragement, academic support, and guidance, all of which have greatly contributed to the successful completion of my project.

My special thanks goes to **Ms. Priyanka Yadav**, Ph.D. scholar, for her continuous support, valuable suggestions, and unwavering motivation throughout the course of this work.

Lastly, I am deeply grateful to my family and friends, whose patience, understanding, and encouragement provided the emotional strength and motivation I needed during long hours of research. Their unwavering belief in me was a constant source of inspiration.

Rachana

ABSTRACT

This study investigates using activated *Calotropis gigantea* (CG) leaves as a natural, cost-effective phytosorbent for the sequestration of crystal violet (CV). The various techniques, including FTIR, XRD, FESEM, DLS, BET, and UV-Vis spectrophotometer, were used to illustrate the efficiency of the phytosorbent. The adsorption behavior of the biosorbent was examined by varying several parameters, such as pH, dye concentration, adsorbent amount, thermodynamics, and equilibrium time. Adsorption isotherms and kinetic models were also fitted. The maximum adsorption capacity of CV on ACG was found to be 111.11 mg/g achieved at 35°C or 308.15 K. The calculated thermodynamic parameters, such as ΔH and ΔS for CV uptake on the adsorbent surface, come out to be 22.397 kJ/mol and -100.25 J/mol/K, respectively. The positive enthalpy change, confirms the endothermic nature of the adsorption process. The negative values of ΔG confirmed the spontaneous nature of the adsorption process. The recyclability of the adsorbent is also good after 4 cycles of regeneration, and the adsorbent has ~80% removal with the real waste water sample. Overall, phytosorbents based on dried Calotropis gigantea leaves demonstrate strong potential as an effective biosorbent for the adsorption of crystal violet via contaminated water.

Keywords: Biosorbent*; Calotropis Gigantea* ; Adsorption; Crystal Violet

Contents

1. INTRODUCTION & LITERATURE REVIEW

Water scarcity is a major concern for living beings. Even though water covers 71% of the surface of the Earth, only 3% of it is suitable for consumption by humans. The major contributors to scarcity may be the rapid expansion of urbanization, globalization, industry, and population. The most common factors contributing to water pollution are agricultural runoff, industrial effluents, and household waste (Musie & Gonfa, 2023). In addition to that, industrial dye effluent poses a distinct threat, and it not only pollutes water bodies but also poses a significant danger to aquatic ecosystems. There are a variety of industries that generate dye-containing waste, including textiles, leather, paper and pulp, plastics, rubber, pharmaceuticals, food, cosmetics, paints, and printing (Ajiboye et al., 2021; Indu Rani, Sudhir Warkar, 2024; Lellis et al., 2019). As a result of their potential toxicity, carcinogenicity, and mutagenicity, these waste products are a serious threat to human health (Elgarahy et al., 2021). It has been reported that dyes produce cyanosis, irritated skin, irreversible blindness, itchy eyes, dizziness, skin staining, and elevated heart rate (Abbasi et al., 2019). Hence, industrial wastewater must be treated before it is released into water sources in order to remove these toxins. Monira and the group have demonstrated that cationic dyes are much more toxic and dangerous in comparison with anionic dyes, due to their interaction with the cytoplasm and hampering the normal physiological functioning of living beings (Ghoniem et al., 2022). The cationic dye, Crystal Violet (CV), comprises a triphenylmethylamine compound with the molecular formula $C_{25}H_{30}N_3Cl$. It is a known genotoxic compound capable of causing mitotoxic poisoning (Ghoniem et al., 2022). Due to its extended environmental persistence and prolonged shelf life, CV is a recalcitrant dye molecule, and CV exposure may cause irritation, redness, and swelling at the site of contact. The adverse effects of crystal violet (CV) exposure include permanent skin discoloration, allergic reactions, dermatitis, and necrosis (Quansah et al., 2020). Even at very low concentrations (0.1-10 mg/L) of CV present in water, it can have significant toxic effects on aquatic life and pose health risks to humans if the contaminated water

is used for drinking or irrigation. Even certain species of fish are also susceptible to this agent, which is a mitotic poison, a potent carcinogen, and a clastogenic agent that promotes tumorigenesis. Hence, CV is considered to be a biohazard (Yadav et al., 2024a, 2024b). The effects of this substance are gradual and persistent on living organisms and the environment. Despite its high chemical stability, this compound has a very low degradation rate, which contributes to its environmental persistence. Considering CV's prolonged environmental stability and potential hazards, we must develop effective methods for degrading it from aquatic systems (Dimbo et al., 2024). Several methods have been used to remove toxic compounds, including membrane filtration, ion exchange, precipitation, coagulation-flocculation, chemical oxidation, ozonation, biosorption, and photodegradation (Ahmed et al., 2022; Shanaah et al., 2023). However, these methods have some limitations, such as high costs, the generation of secondary waste that is difficult to handle, prolonged processing times, and limited reusability. Adsorption has emerged as a preferred method to remove dye because of its ease of application, cost-effectiveness, simplicity, versatility, and environmental sustainability (Dutta et al., 2021; Yusuff, 2022). For adsorption, various materials can be employed, including nanoparticles, carbon-based materials, biomaterials, polymeric materials, and biomass waste-derived sorbent (Bayramoglu et al., 2020; Bayramoglu & Arica, 2021; Yang et al., 2019). Hence, developing low-cost adsorption materials with high uptake capacities is essential. In consequence, treating wastewater, plant derived waste materials, and waste from agricultural land may serve as a scavenger for dye removal with numerous benefits, such as biocompatibility, bioavailability, biodegradability, ease of synthesis, etc, for dye sequestration (Arica et al., 2022; Xu et al., 2022). There are several distinct advantages to using these materials, such as their accessibility, nontoxicity, and environmental sustainability (Al-Asadi et al., 2023; Dimbo et al., 2024). There is significant amount of organic waste generated every year, including seeds, fruit peels, stems, leaves, flowers, shells, biomass, and grasses. In spite of their low economic value, their utilization as phyto-sorbents holds significant

environmental promise, transforming them into valuable pollution control and waste management resources (Mahato et al., 2022; Mohanta et al., 2021; Rout et al., 2022; Tahir et al., 2016). The Leaf-derived adsorbents exhibit high efficacy in dye removal owing to their unique composition, which encompasses cellulose, polyphenols, hemicelluloses, pectin, and lignin (Mahato et al., 2022; Qaiyum, Mohanta, et al., 2022) Additionally, these materials are typically enriched with functional groups such as hydroxyl, carboxyl, amino, and carbonyl groups. These functional groups serve as active adsorption sites, significantly enhancing the dye-binding capacity of leaf-based adsorbents. Therefore, a lot of biomass-derived biosorbents like peepal leaf, orange peel, coconut fiber, and eucalyptus leaf-based sorbents have been tested and utilized as green sorbents (Akl et al., 2021; Das et al., 2024; Doan Thi et al., 2020; Qaiyum, Sahu, et al., 2022; Rani et al., 2017).Modified rubber seed pericarp biomass-based adsorbent for the removal of crystal violet and methylene green (Uddin et al., 2023). Marahel and the group have utilized Albizia stem bark lebbeck-based adsorbent for the removal of methyl violet using response surface methodology (Einolghozati et al., 2022). Similarly, Abbas and the group have used a neural network model to sequestrate methyl paraben using Ricinus Communis capped FeNPs as an adsorbent (Marahel, Farzaneh*+; Mombeeni Goodajdar, Bijan; Basari, Neda; Niknam, Leila; Ghazali, 2022). While Niknam and the group have used RSM as well as ANN for the scavenging of reactive yellow 105 dye using Zeolitic Imidazolate-67 modified by Fe_3O_4 dye (Pournamdari et al., 2024) Calotropis gigantea, commonly known as ‘Akh’, belongs to the family of Apocynaceae. This species is indigenous and often found growing in wastelands and roadside areas. The plants have various bioactive compounds like flavonoids, terpenoids, and phenolic compounds, which contribute to their utilization in traditional medicines and industries. Beyond these applications, recent studies have highlighted the potential of the Calotropis gigantea plant’s fibre as an effective biosorbent for environmental remediation. The natural functional groups present in the leaves can bind and remove pollutants, including dyes and toxic compounds, from contaminated water (Belmabrouk et al., 2023). However, except for

the fibre of CG, other parts of plants are not explored for the crystal violet dye, which is a common hazardous pollutant in textile wastewater, remains unexplored, and forms the focus of the present study (Yadav et al., 2025). While various adsorbents have been investigated for the removal of crystal violet (CV) dye from aqueous systems, many rely on synthetic, costly, or non-renewable materials that limit their practical application. The removal of synthetic dyes such as Crystal Violet from wastewater is critical due to their toxicity, persistence, and potential harm to aquatic ecosystems and human health. The developed adsorbent offers an efficient, cost-effective, and eco-friendly solution for dye removal, minimizing the release of hazardous pollutants into the environment. By effectively reducing dye concentrations in contaminated water, this work contributes to mitigating water pollution and supports sustainable water management practices. Furthermore, the use of readily available and possibly renewable materials for adsorbent preparation enhances the environmental compatibility of the treatment process. To the best of our knowledge, indigenous Calotropis gigantea, an indigenous and readily available plant, has not been previously explored for the sequestration of crystal violet (CV) dye from aqueous systems. This lack of research represents a significant gap, as utilizing locally available biomass can provide a cost-effective and sustainable alternative for dye removal in wastewater treatment. Therefore, the primary goal of this study is to develop and evaluate a phyto-sorbent derived from the alkali-modified leaves of CG for the efficient adsorption of CV dye from water. This work aims to assess the adsorptive performance through a systematic investigation of key physicochemical parameters such as contact time, pH, adsorbent dosage, initial dye concentration, and the impact of temperature. The ultimate objective is to demonstrate the potential of abundant waste plant material with chemical modification for better adsorption efficiency, which offers a low-cost, sustainable bio sorbent as an effective, scalable alternative to conventional materials for wastewater treatment.

2. MATERIALS AND METHODS

2.1 Materials and Instruments

Calotropis gigantea (CG) (Akh) plant leaves were collected from a rural area of Samaypur Badli, Delhi, India, located at approximately 28.7383° N latitude and 77.1324° E longitude. CV (≥ 90%), Methyl Orange (MO) (≥85%), and Methylene blue (MB) (≥ 85%), dyes were obtained from Thermo-Fischer, India. Sodium hydroxide (NaOH) (97%), ethanol (99%), and acetone (99%) were purchased from Sisco Research Laboratory (SRL) Chemicals, Delhi, India. Hydrochloric acid (HCl) (35-38%) Central Drug House (CDH), India. All the studies were conducted in distilled water. FTIR spectra were obtained using PerkinElmer FTIR spectrometer, USA (400-4000 cm^{-1}). PXRD analysis was done by Bruker D8 Advanced X-ray diffractometer, Germany ($2\theta = 5–70°$) with Cu Kα radiation ($\lambda = 1.5418$ Å). FESEM images were obtained using JEOL JSM 6610LV, Japan. BET-BJH analysis for specific surface area and pore size distribution was done using a Quanta Chrome Nova Win at 77 K, Japan. Zeta potential was measured via DLS using a Malvern Zeta sizer Nano-ZSP, UK. UV–vis absorption spectra were used to record dye concentration at λ_{max} = 578 nm at room temperature using a Shimadzu UV–Vis 1900i spectrophotometer, Japan. Solution pH was maintained using Eutech Scientific Thermo Fischer, India. All the experiments were conducted three times to check the reproducibility of the adsorbent. The statistical analysis was done, and the error bar was inserted in the figures of experimental data. Error bars shown in the figures represent the standard deviation of at least three independent experimental replicates, providing a measure of reproducibility and variability in the data. These bars highlight the consistency of the adsorption performance. The relatively small error margins indicate the robustness of the developed platform for dye removal. Including error analysis ensures statistical confidence in the observed trends and supports the reliability of the proposed mechanism." (mean ± SD) using a one-way analysis of variance (ANOVA) ($p < 0.05$) was determined to be statistically significant. This rigorous error analysis provides

statistical confidence in the observed trends and supports the validity of the proposed adsorption mechanism.

3. EXPERIMENTAL SECTION

3.1 Synthesis

3.1.1 Collection and preparation of activated calotropis gigantea (ACG)

Initially, calotropis gigantea (CG) leaves were detached from the stems, which were collected from nearby areas of our university in November 2024. The leaves were first washed with tap water, followed by distilled water to remove dirt and other impurities. Then, the leaves were sun dried for two days to remove the moisture, followed by oven drying at 60 °C. The dried leaves were then crushed into powder using a regular mixer grinder. The obtained crushed powder of leaves was then sieved to obtain a fine powder and stored in an airtight container, which was further projected to alkali activation. Further, for the activation of CG, 1 g of CG was suspended in 50 ml of 1 M NaOH solution and stirred overnight, as presented in Figure 1. The activated CG was then filtered out and neutralized till the pH 7 was attained and then left for drying at ambient temperature to get the desired adsorbent which was utilized to adsorb the crystal violet dye from the aqueous medium.

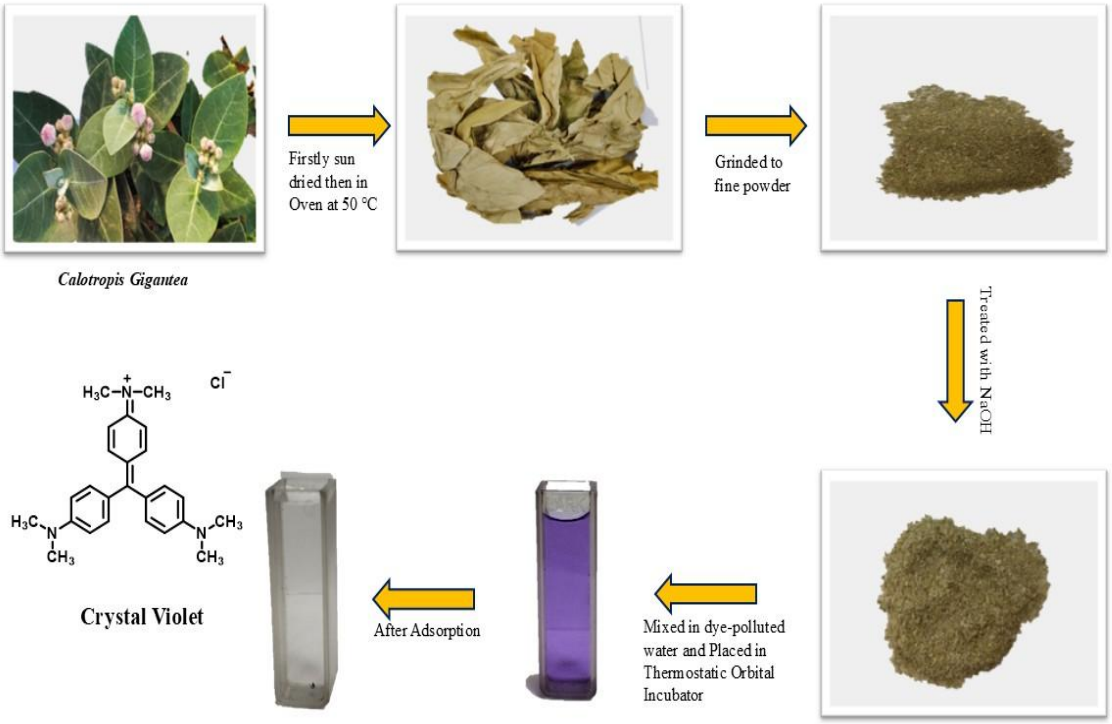

3.2 Batch analysis

To illustrate the adsorption efficiency, the batch study of ACG was carried out at 35° C. To perform the contact time study, 0.1g of alkali-modified CG was dissolved in 50 mL of crystal violet (CV) of concentration 40 (mg/L). The solution was agitated in an orbital shaking incubator at a speed of 100 ± 10 for 60 min. The pH was adjusted using 1M NaOH and 1 N HCl solution, and the study was performed at pH 8.5. After a fixed interval of 10 min, 3 mL of the sample was taken out, and CV dye concentration was recorded using a Shimadzu UV vis spectrophotometer at λ_{max} = 580 nm. Similarly, pH study, adsorbent dosage, dye concentration, and effect of temperature were studied. To calculate maximum equilibrium adsorption capacity (qe), and adsorption percentages (% R), using the below equations (1) and (2):

$$\% R = \frac{C_i - C_f}{C_i} \times 100 \qquad (1)$$

$$q_e = (C_i - C_f) \times \left(\frac{V}{W}\right) \qquad (2)$$

3.3 Isotherms

The interaction between the dye and the adsorbent surface can be evaluated through adsorption isotherms, which illustrate how the dye interacts with the adsorbent surface at equilibrium.

The Langmuir isotherm is attributed to the monolayer adsorption of dye onto a homogeneous surface, assuming negligible intermolecular repulsion between the adsorbed molecules. The adsorption sites are equally active and localized, with no influence of neighboring sites on the dye binding process. The linearized equation of the model is presented in the equation (3) (Ayawei et al., 2017). The linear equation for the Langmuir model is:

$$\frac{c_e}{q_e} = \frac{1}{k_L q_{max}} + \frac{c_e}{q_{max}} \qquad (3)$$

where q_{max} (mg g-1) represents the maximum adsorption capacity and q_e (mg g^{-1}) represents the equilibrium adsorption capacities of CV, respectively. While, C_e (mg L^{-1}) represents equilibrium concentrations of CV and K_L (L mg^{-1}) is the Langmuir constant.

R_L is a unitless constant that is used to determine linearity (R_L=1), irreversibility (R_L=0), favourability (0 < R_L <1) of adsorption and is calculated with the given formula-

$$R_L = \frac{1}{1+k_L C_i} \qquad (4)$$

Where CV solution concentration (mg L^{-1}) is given by C_i.

The Freundlich model mainly correlates with heterogeneous surfaces, and the adsorption equilibrium in multi-phase adsorption surfaces is not homogeneously distributed on the surface of the adsorbent. The linearized form of the model is expressed as (Freundlich, 1907).

$$\log q_e = \log K_f + \frac{1}{n_f} \log C_e \qquad (5)$$

$$q_e = K_f \times C_e^{\frac{1}{n_f}} \qquad (6)$$

here, q_e refers to adsorption capacities (mg g-1), and Ce represents the equilibrium concentration of CV dye (mg L^{-1}). While Freundlich coefficients, K_f [(mg g^{-1}) (L mg^{-1})

1 /n_f represents the adsorption capacity of adsorbate, and n_f indicates heterogenic adsorption intensity.

The Temkin model suggests that as the coverage of the adsorbate on the adsorbent decreases, the heat of adsorption also decreases across the entire molecule. This model describes the uniform binding of the adsorbate to the surface of the adsorbent, and it also demonstrates that the decrease in adsorption heat for the molecules fits a linear pattern, supporting homogeneous binding energy (Mori & Maksimov, 1999).

$$q_e = \frac{RT}{b} \ln A + \left(\frac{RT}{b}\right) \ln C_e \qquad (7)$$

RT/b = BT, Where R is the gas constant (8.314 J mol^{-1} K^{-1}), T is the absolute temperature in Kelvin (K), and B represents the heat of adsorption (J mol^{-1}).

3.4. Kinetics

The interaction mechanism between the adsorbent and adsorbate along with the reaction rate, was analyzed using three kinetic models: the pseudo-first-order model, the pseudo-second-order model, and the Elovich model. According to the pseudo-first-order model, the rate of adsorption is directly proportional to the number of active vacant sites on the adsorbent's surface. The linear expression as (Musah et al., 2022).

$$\ln(q_e - q_t) = \ln q_e - K_1 t \qquad (8)$$

Here, q_e and q_t are the adsorbent uptake capacity (mg g^{-1}) of dye at equilibrium and at a time 't.' K_1 is rate constant (min^{-1}).

The pseudo-second-order kinetic equation assumes that the rate of site occupancy is proportional to the square of the unoccupied sites, as shown in linear forms (Bullen et al., 2021):

$$q_t = \frac{k_2 q_e^2 t}{1 + k_2 q_e t} \qquad (9)$$

Here, q_e and q_t (mg g^{-1}) represent the dye uptake of adsorbent at equilibrium and at the time 't'. The rate constant is determined by k_2 (min^{-1}). The initial adsorption rate 'h' (mg g^{-1} min^{-1}) can be determined by the equation:

$$h = k_2 q_e^2 \qquad (10)$$

Elovich's model is based on the assumption that the adsorption rate decreases exponentially as the amount of adsorbed solute increases. Adsorption-desorption kinetics was given by linear expression using the Elovich model (Wu et al., 2009).

$$q_t = \frac{1}{\beta}\ln(\alpha\beta) + \frac{1}{\beta}\ln t \qquad (11)$$

$$q_t = \beta \ln(\alpha\beta t) \qquad (12)$$

Here, q_t (mg g^{-1}) uptake capacity of dye at the time 't,' α is the initial rate of adsorption (mg g^{-1} min^{-1}), and β is the desorption constant (g mg^{-1}). If the value of α is greater than β, it implies that the chemical sorption occurs between the adsorbate and adsorbent phases. Kinetic modeling of experimental data involves determining the rate of adsorption in a system.

4. RESULT AND DISCUSSION

4.1 CHARACTERISATION

4.1.1. Fourier Transform Infrared Spectroscopy

The FTIR spectra of CG and ACG is presented in Figure 2, which provide insights into the functional groups present on their surface. It was found that no significant difference was

observed in the FTIR spectra of CG and ACG (Bora & Karak, 2022). In CG, the broadband at 3290 cm^{-1} corresponds to hydroxyl (O–H) groups associated with cellulose and lignin, while the intensity of this peak is reduced in ACG due to dehydration and reduction of hydroxyl group after activation, and it was found to be at 3289 cm^{-1} (Yahya et al., 2022). The peaks at 2918 cm^{-1} and 2846 cm^{-1} are attributed to the asymmetric C–H vibrations of alkyl groups, while the intensity of this peak is less prominent in ACG, indicating the decomposition of volatile organic compounds during activation (Sun et al., 2020). The bands at 1600 cm^{-1} and 1241 cm^{-1} confirm the presence of C=O and C=C aromatic groups in hemicellulose and lignin. While in ACG, there is a little shift in these peak positions may be attributed to that partial oxidation and may be a modification in the carbonyl group. The peak at 1414 cm^{-1} is associated with C–H bonds in cellulose, while the peak at 1015 cm^{-1} attributed to C–O–C stretching vibrations in cellulose while less prominent peaks present in ACG may be attributed to the disruption of polysaccharide structure present in ACG which may lead to enhancement of carbon content resulting higher surface area and thereby enhanced adsorption in ACG (Kaur & Kaur, 2017).

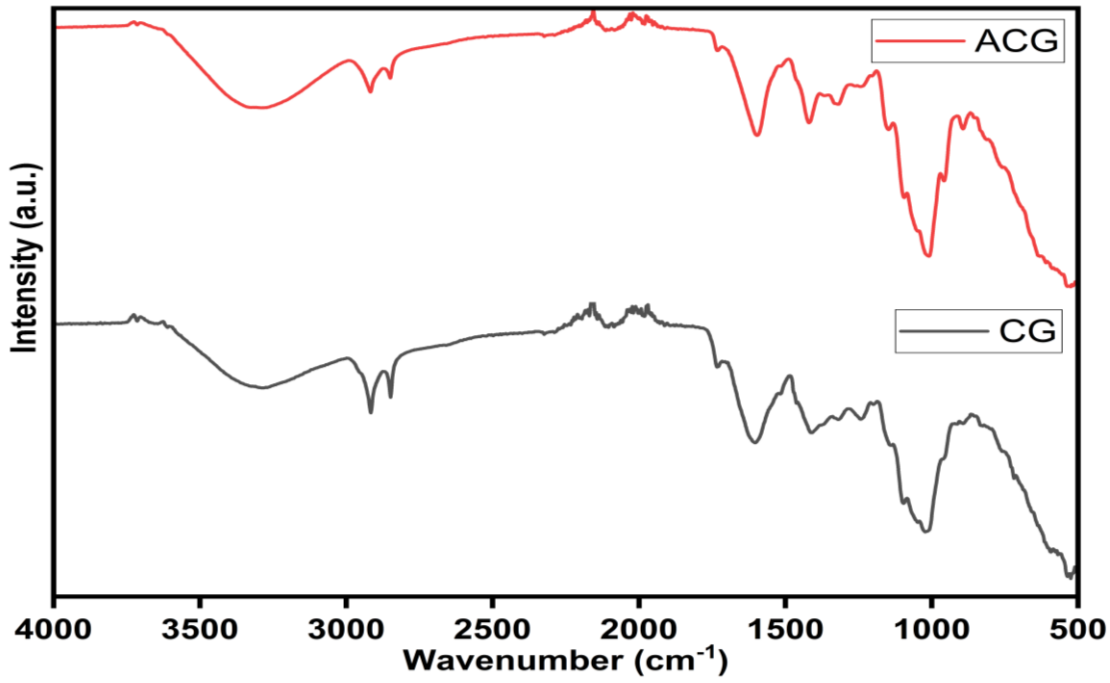

Figure 2 . FTIR plot for ACG and CG

4.1.2 .X-Ray Diffraction

The XRD pattern of CG and ACG is presented in Figure 3. The XRD pattern of CG represents a principle peak at 22.42°, attributed to the semi crystalline cellulose present in CG. The presence of minor sharp peaks in CG associated with residual of inorganic components present in CG. While, more pronounced broad band in ACG was found at 20° and loss of minor crystalline peaks are diminished suggested the amorphous nature occurred due to chemical activation of CG. Hence, it may be concluded that activation leads to breakdown of cellulose and lignin present which may lead to enhancing the active surface area (Kaur & Kaur, 2017).

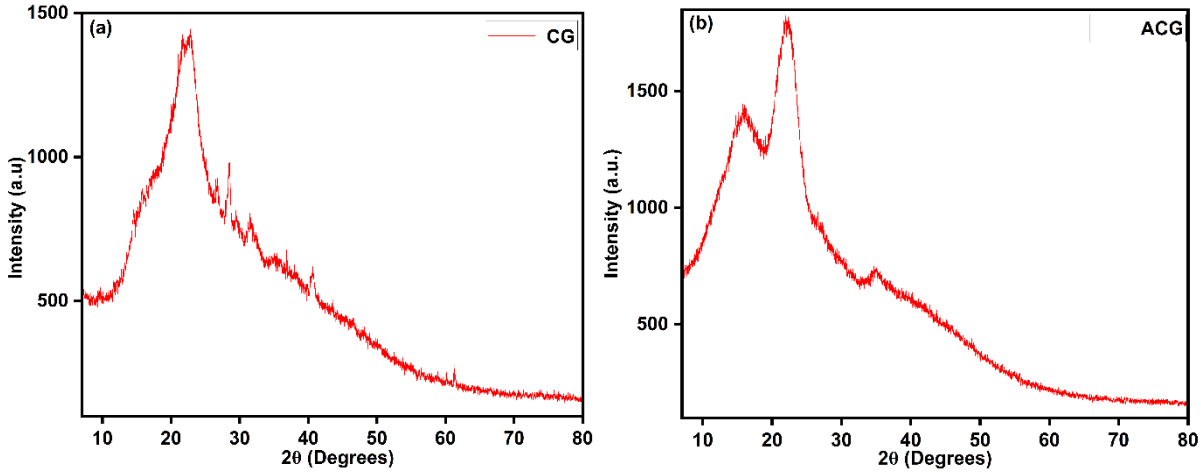

Figure 3. XRD plot of (a) CG and (b) ACG

4.1.3. FESEM

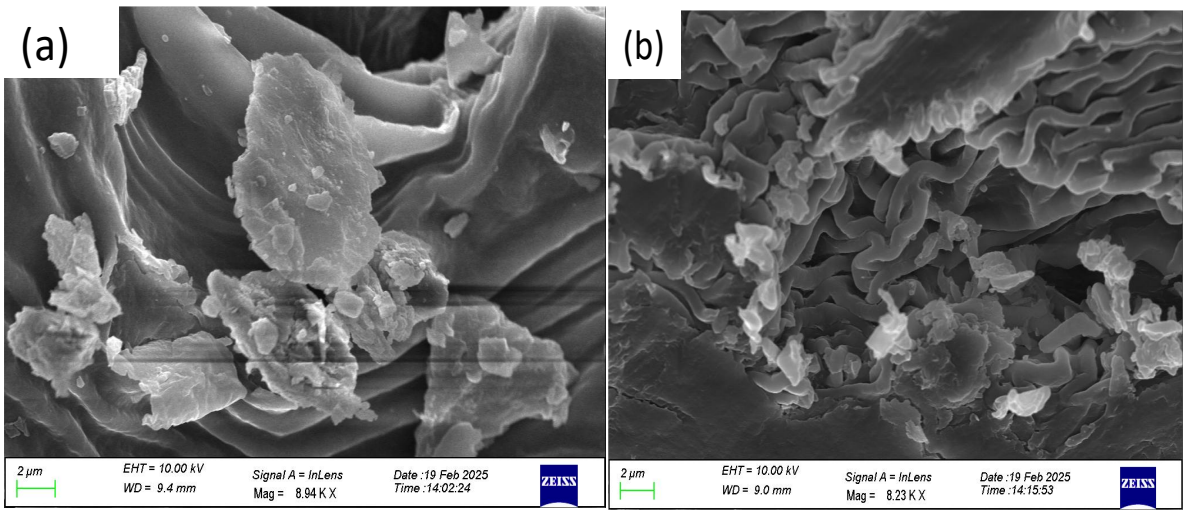

Figure 4. FESEM micrographs of (a) CG and (b) ACG

The micrographs of CG and ACG are presented in Figure 4. In CG, layered, smooth, and irregular large particles were present, while in ACG, comparatively rough surface and more porous fragmented morphology are observed, which may result in more adsorption sites resulting in comparatively higher adsorption in ACG.

4.1.4. Dynamic Light Scattering

The dynamic light scattering method is used to find out the zeta potential of the sorbent presented in Figure 5. The zeta potential will provide information about the stability and the charge of the sorbent. In CG, a slightly negative potential was found, which may lead to less electrostatic interaction, while in ACG, an increase in negative surface charge leads to enhanced electrostatic interaction, which may help to more pronounced adsorption of dye molecules over the sorbent surface.

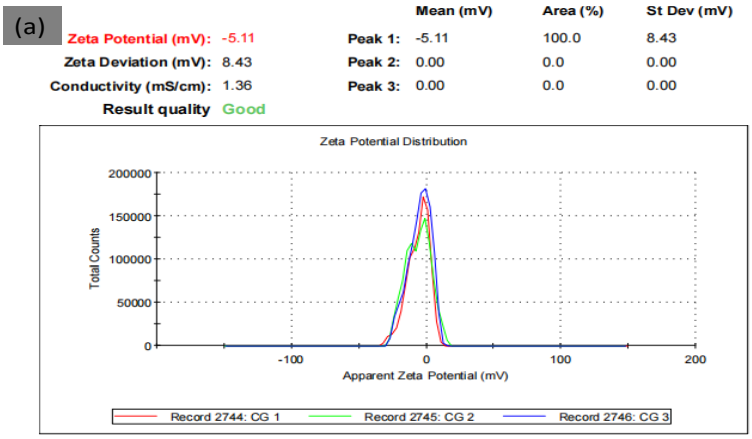

Figure 5. Zeta potential of (a) CG and (b) ACG

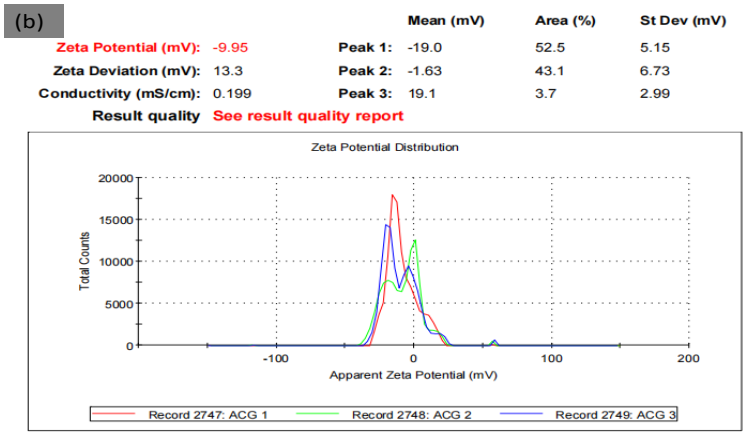

4.1.5 BET

The surface area of CG and ACG were estimated using Brunauer Emmet-Teller (BET) analysis and found to be 4.719 m^2/g and 8.097 m^2/g, respectively presented in Figure 6. The pore volume for CG and ACG were measured using the BJH method and was found to be 0.004 cc/g and 0.005 cc/g, respectively, and the pore radius was found to be 15.288 Å and 19.142 Å, respectively. Therefore, it is concluded that upon alkali activation, the surface area of CG increased, allowing for increased adsorption in ACG. It was observed that the Type IV isotherm for CG and the Type I isotherm for CG were observed which suggest that mesoporous and microporous material.

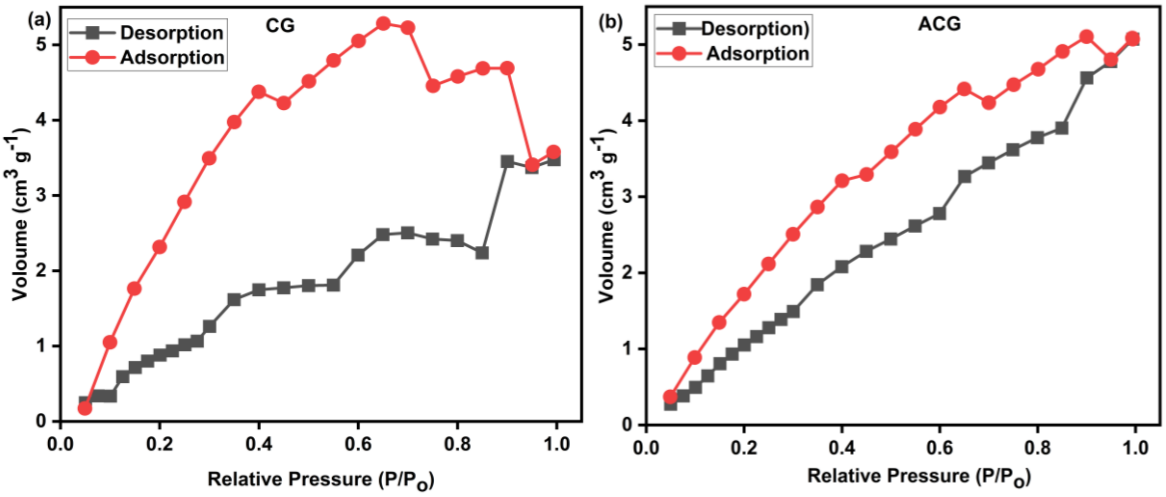

Figure 6. N_2 adsorption-desorption BET analysis of (a) CG and (b) ACG

4.2 Adsorption Studies

4.2.1 Impact of equilibration time

The contact time in adsorption studies is greatly affected by the contact time of an adsorbent and a dye solution, which provides information about the equilibriums of the reaction. The % dye adsorption of CV dye using ACG is depicted in Figure 7. Initially, as the process of adsorption started, the % dye adsorption was found to be 64% in 15 minutes, which further increased to 92.6% in 60 minutes. It was observed that there is no significant difference in % dye adsorption

after 60 minutes, which may suggest that the adsorbent is saturated. This may be attributed to the fact that the adsorption sites were readily available in the initial stages, resulting in faster adsorption [29]. As time increases, a lesser no. of vacant sites on the adsorbent surface remains, suggesting saturation has been reached. Therefore, for all other experiments the contact time was taken as 60 minutes **.**

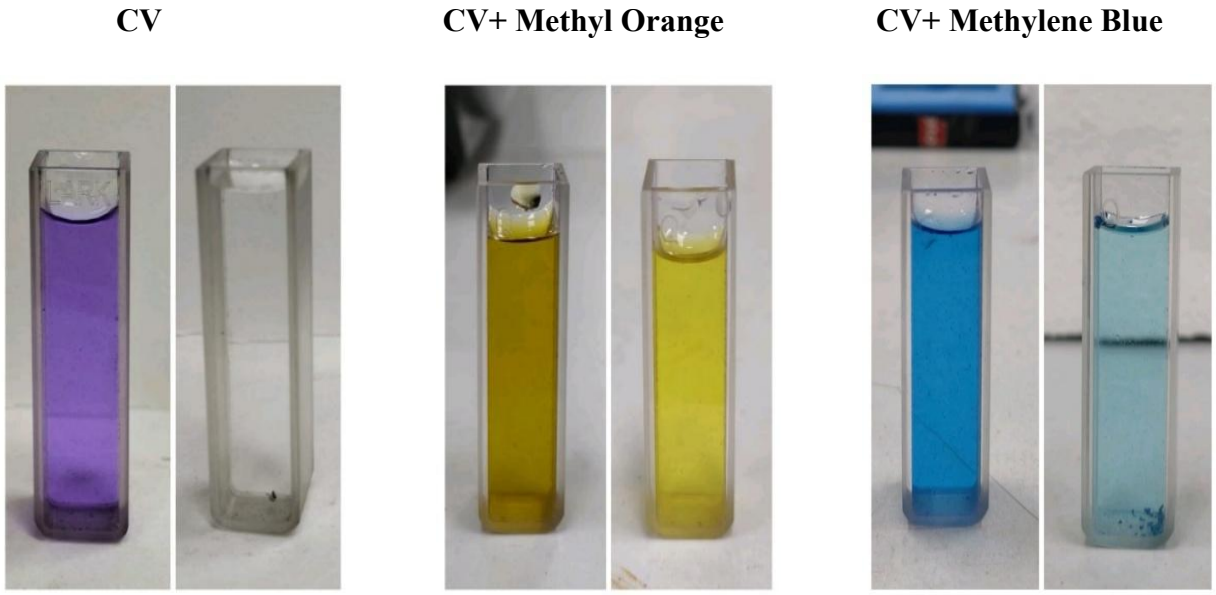

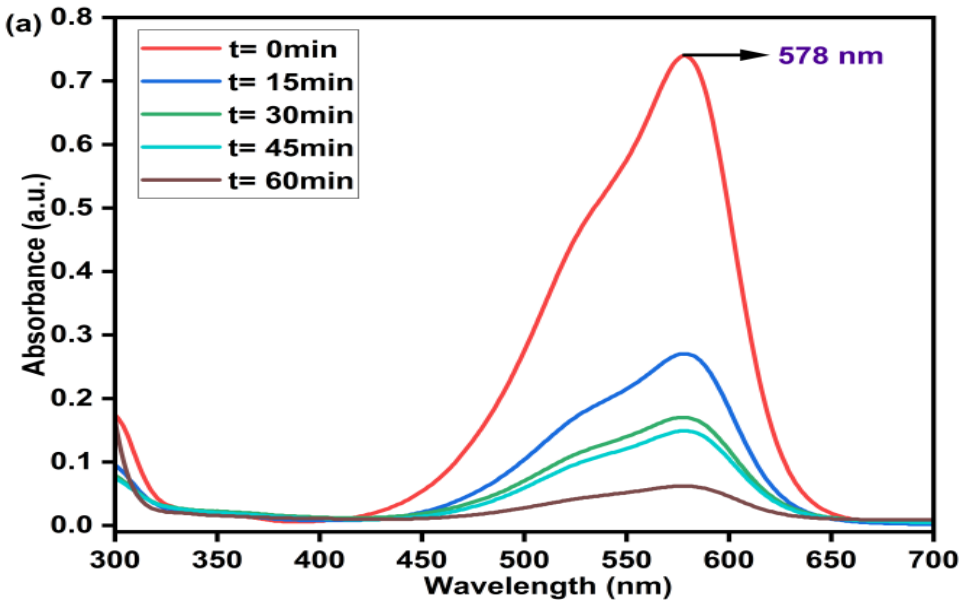

Figure 7. (a) Plot of UV-visible adsorption spectra

(b) Plot of percentage (%) of dye adsorption using ACG.

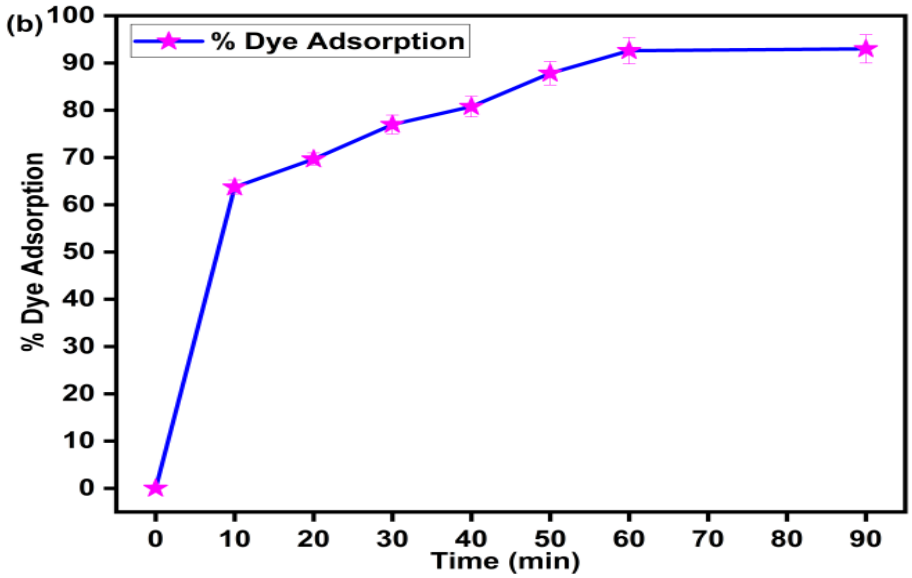

4.2.2 Impact of adsorbent dosage

The dosage study was performed to optimize the amount of adsorbent. To perform this, 0.025 0.15g of adsorbent was taken in 50 mg/L of CV dye, which can be seen in Figure 8. It was found out that as the dose of adsorbent increased from 0.025g to 0.1g, the % dye adsorption increased from 70 to 92.59%. The reason behind this may be that increasing the quantity of adsorbent results in greater surface area; thus, more active sites are vacant to adsorb the dye onto the adsorbent surface (Belmabrouk et al., 2023). While on further increment in the dosage amount of 0.15g, then the dye adsorption was found to be 89%. This may suggest that the decrease in % dye adsorption with increasing sorbent amount may be due to some of the available adsorption sites remaining unsaturated during the adsorption process because the higher number of adsorbent molecules interacting itself and hinders the interaction of dye onto the adsorbent surface, leading to the decrease in adsorption (Pathak & Singh, 2023a). Thereby, the higher the amount of adsorbent, the lesser the interaction of the dye molecule onto the adsorbent surface.

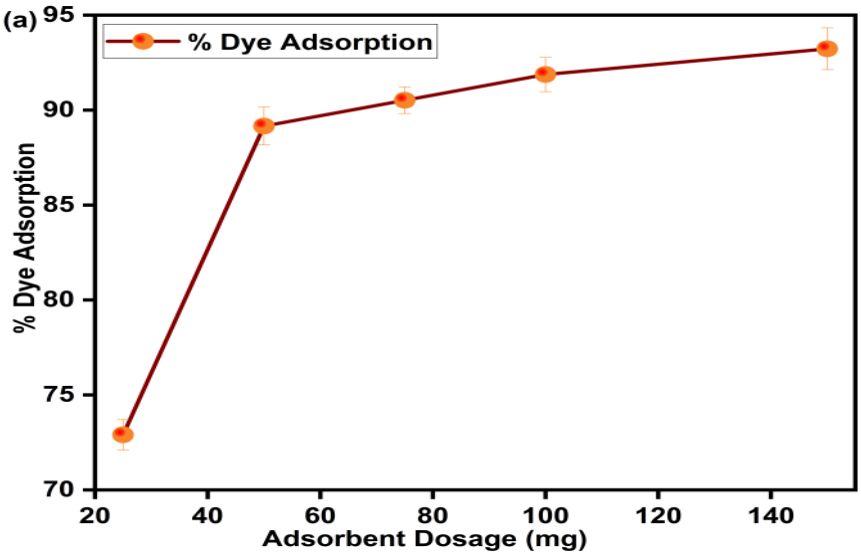

Figure 8: Impact of adsorbent dosage

4.2.3 Impact of pH

The pH of the solution plays a significant role by altering the surface charge density on the adsorbent as well as the ionizing power and controls the interactions between the adsorbent and adsorbate. The impact of pH on CV adsorption by ACG was monitored in the range of pH 5.5-9.5, with 0.1g of adsorbent and 60 min of reaction time, as presented in Figure 9. It was observed that on increasing pH from 5 to 10, % dye adsorption was initially increased up to pH 9 from 86% to 92.59%. On increase in pH, a decreament in % dye adsorption was observed. This can be correlated with the (pH_{ZPC}) zero-point charge, which was found to be 7.63. The pH_{ZPC} value determines the surface charge of the adsorbent in relation to the solution's pH, presented in Figure 9c. When the pH of the solution is less than pH_{ZPC}, the adsorbent surface acquires a positive charge, while at pH values more than pH_{ZPC}, the surface becomes negatively charged. This behavior arises because, at lower pH levels ($pH < pH_{ZPC}$), the excess H^+ ions in the solution lead to protonation of the adsorbent surface (Akpomie & Conradie, 2023). Conversely, at higher pH levels ($pH > pH_{ZPC}$), the abundance of OH^- ions in the solution imparts a negative charge to the adsorbent surface (Issabayeva et al., 2022). As pH decreases, protonation occurs on the CG surface, which repels the cationic dye CV, thus preventing dye molecules from adhering to the

surface. On increasing the pH, the surface of ACG becomes negatively charged, which favours cationic dye binding due to electrostatic attraction, increasing adsorption.

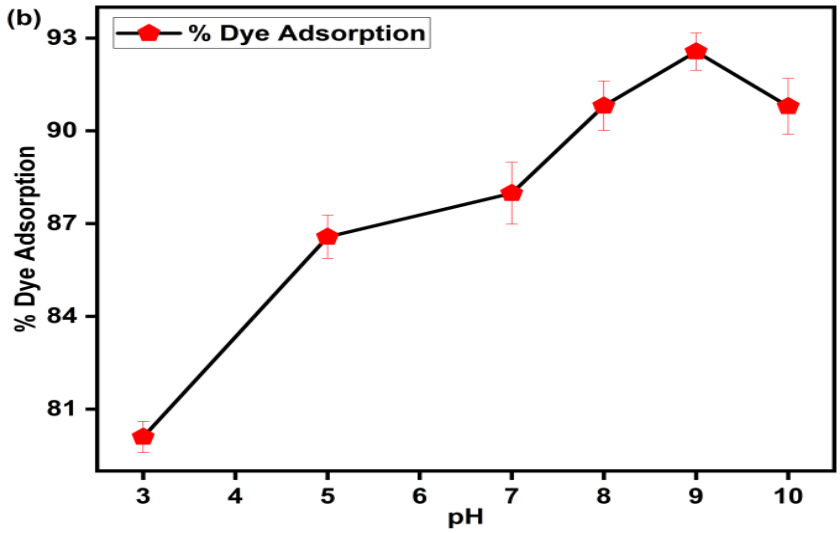

Figure 9a: Impact of pH

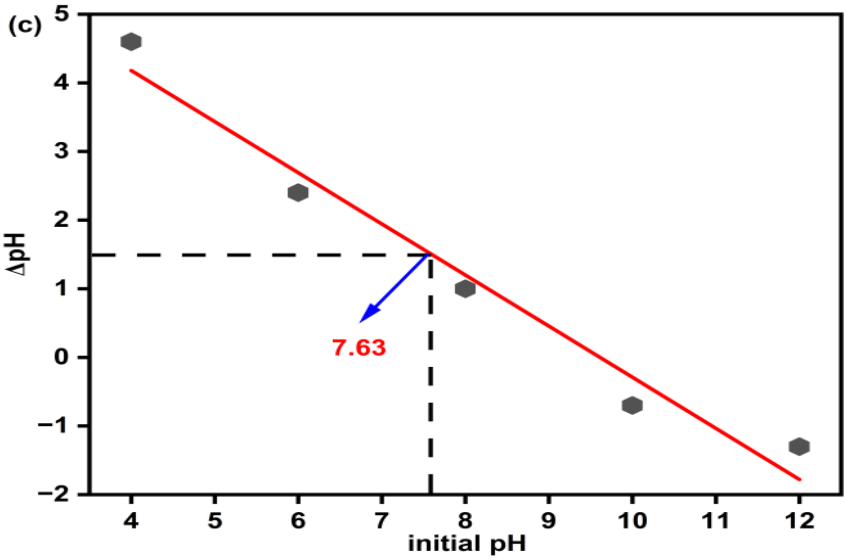

Figure 9b: Point zero charge (pH_{ZPC}) on adsorbent

4.2.4 Impact of Dye Concentration

The effect of dye concentration variation from 20 mg/L to 100 mg/L is presented in Figure 5a. The impact of concentration was studied on the % dye adsorption, and it was noticed that as the concentration of dye rose from 20 mg/L to 100 mg/L, % dye adsorption decreased from 92.59 % to 77%. It may be concluded that due to the lower concentration of dye, dye molecules are lesser

and may easily adsorb on the synthesized adsorbent, while on the higher side of dye concentration, a saturation of active sites has been reached due to excessive CV molecules available in the solution (Pandey & Singh, 2023; Pathak & Singh, 2023b). In addition, it showed an increase in equilibrium adsorption capacity (q_e) from 36.63 to 168 mg/g when dye concentration increased, showing that equilibrium adsorption capacity is also increased presented in Figure 10a. Kanishka and the group have reported a similar result (Yadav et al., 2025). An increase in mass transfer from solution to solid may be attributed to a higher concentration because it increases the probability of molecular collisions with adsorbent surfaces. Due to more collisions in the solution phase, molecules are removed at a faster rate. As a result of the higher initial dye concentration, the concentration slope between the dye solution and the adsorbent phase is higher, increasing the adsorption rate.

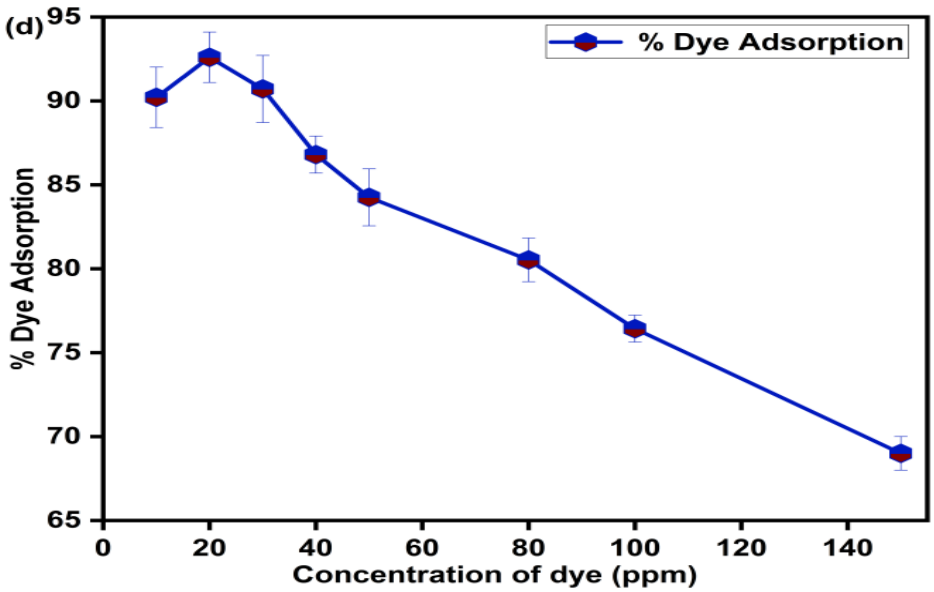

Figure 10a impact of concentration variation on (%) of dye adsorption using ACG.

4.3 Isotherm

Figure 11 shows isotherm plots for the uptake of CV on the phytosorbent ACG, and computed values are presented in Table 1. Experimental data for the uptake of CV using ACG was found to best fit with the Langmuir model, with $R^2 = 0.98$ for CV, suggesting homogeneous monolayer

adsorption on the adsorbent surface. The R_L was calculated to be 0.2. The q_{max} represents the maximum amount of dye adsorbed per unit weight of adsorbent to form a complete monolayer on the surface (mg g^{-1}), and dye sorption capacities (q_{max}) were calculated based on the Langmuir isotherm model. Hence, the q_{max} of the adsorbent was calculated using the Langmuir isotherm, and it was found to be 111 mg g^{-1} for CV (20 mg L^{-1}).

Table 1. Calculated Parameters using Various Models.

Models	**Slope & Intercept**	**Parameters**	**Parameter value**
Langmuir	Slope = 0.009 Intercept =0.024	R^2	0.98
		q_m (mg g^{-1})	111.11
		K_L (L mg^{-1})	0.375
		R_L R_L=1, linearity R_L=0, irreversibility $0 < R_L < 1$, favourability o un-favourability ($R_L > 1$)	0.2
Freundlich	Slope = 0.366 Intercept = 3.5	R^2	0.82
		K_F (mg g^{-1}) (L mg)$^{1/n_f}$	3162.278
		$1/n_f$	0.366
Temkin model	Slope = 24.29 Intercept = 25	R^2	0.898
		B (J mol^{-1})	93.44
		A_T (L g^{-1})	2.79

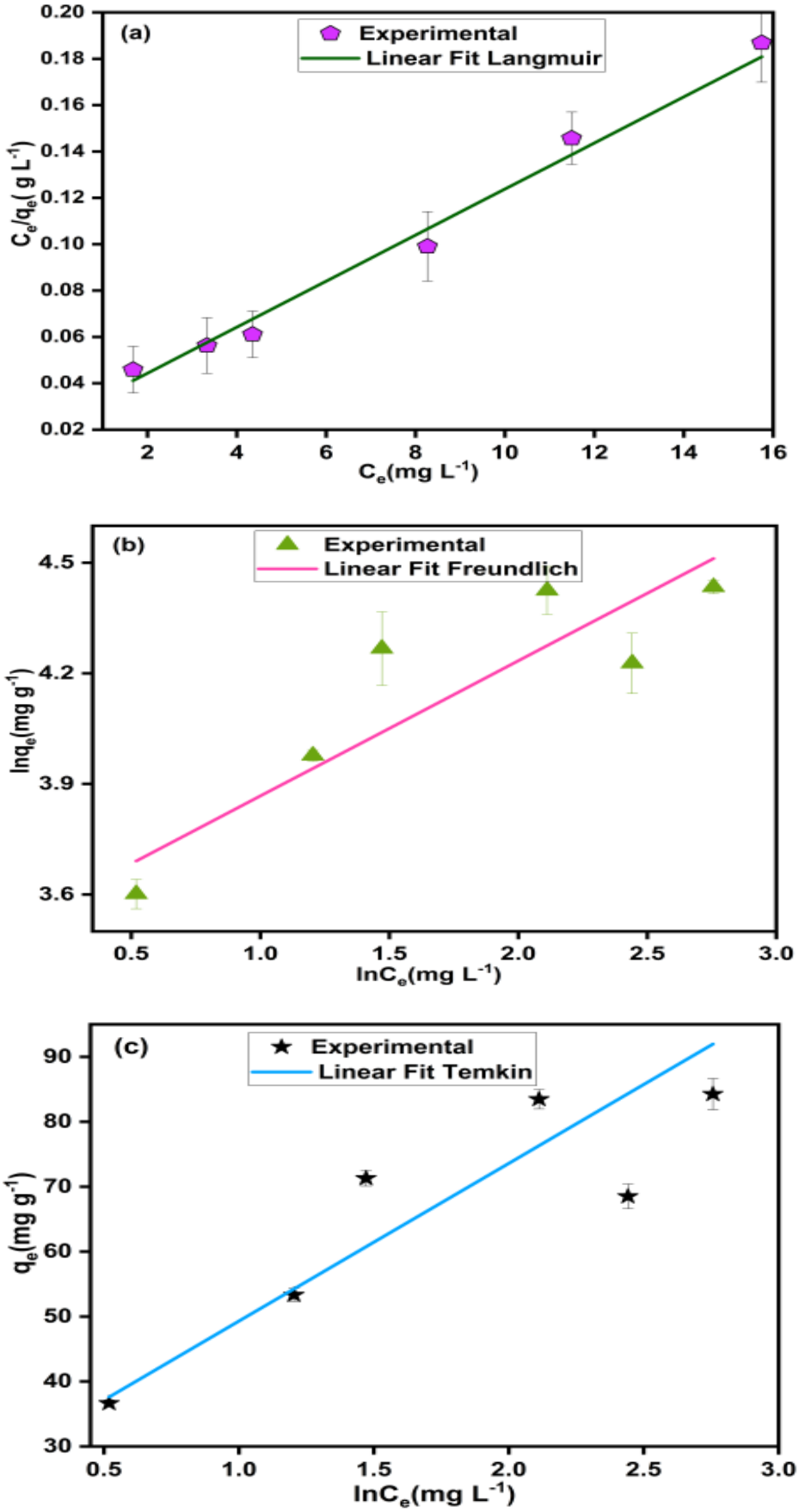

Figure 11. Isotherm plots for (a) Langmuir, (b) Freundlich, (c) Temkin Model.

4.4 Kinetics

To illustrate the mechanism of adsorption, experimental data is correlated with the above-discussed kinetic models. The plots presented in Figure 12 show the linear regression of experimental data with the kinetic models, and the calculated parameters are presented in Table 2. It was observed that the experimental data is in good agreement with the pseudo-second-order model ($R^2 = 0.998$) for CV, suggesting that chemical adsorption is the rate-determining step in dye uptake by synthesized sorbent. The value of h was calculated to be 8.846 mg g^{-1} min^{-1} for CV. Thus, the adsorption of CV on ACG may comprise three steps: (i) initial physical sorption, (ii) chemical sorption, and (iii) possible saturation at the equilibrium stage.

Table 2. Calculated Parameters using Various Models. The data presented by the mean ± standard deviation ($P < 0.05$)

Kinetics Models Plots	**Slope**	**Intercept**	**Values of Parameters**	
First order: $\ln(q_e - q_t) = \ln q_e - K_1 t$ K_1 is rate constant	0.011	3.502	R^2	0.872
			K_1 (min^{-1})	0.011
			q_e (mg g^{-1})	33.18
Pseudo-second order: $\frac{t}{q_t} = \frac{1}{k_2 q_e^2} + \frac{t}{q_e}$ k_2 is the rate constant $h = k_2 q_e^2$; h is initial adsorption rate	0.028	0.113	R^2	0.998
			K_2 (g mg^{-1} min^{-1})	0.007
			q_e (mg g^{-1})	0.028
			h (mg g^{-1} min^{-1})	8.846
Elovich model: $q_t = \beta \ln(\alpha\beta t)$	5.617	11.166	R^2	0.846
			α (mg g^{-1} min^{-1})	1.299
β is the desorption constant, i			β (g mg^{-1})	5.617

α > β, implies chemical sorption				

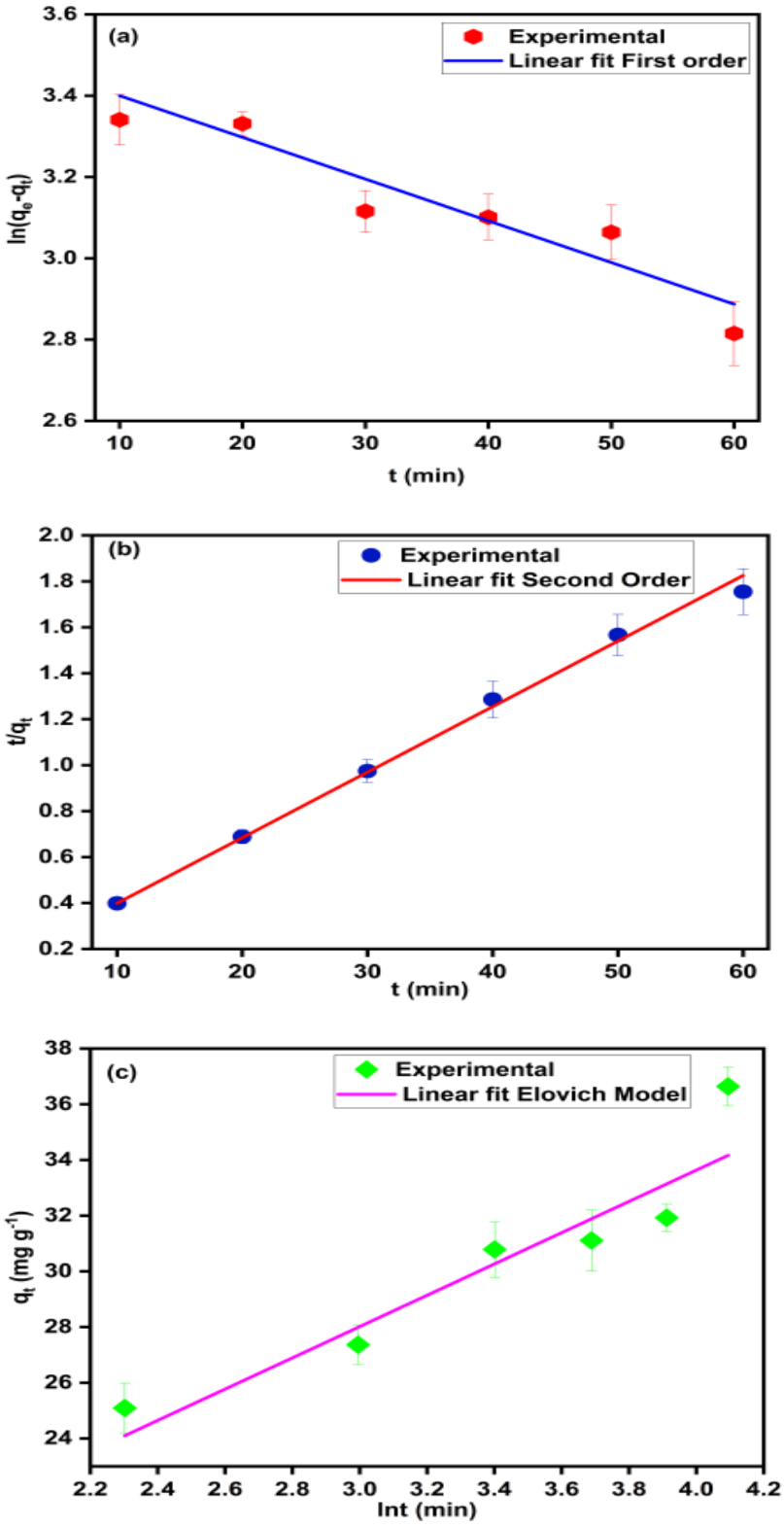

Figure 12. Kinetic Plots for (a) First Order, (b) Second Order, (c) Elovich Model.

4.5 Impact of temperature

The temperature plays a significant role in the % dye adsorption on the adsorbents. The adsorption of CV dye by ACG was investigated by varying temperatures with an interval of 10°C having other parameters similar to the contact time study. The thermodynamic parameters enthalpy, entropy, and free energy were evaluated using the following equations-

$$k_e = \frac{q_e}{C_e} \qquad (13)$$

$$\Delta G^0 = -RT\, ln\, K_e \qquad (14)$$

$$ln\, K_e = \frac{\Delta S^0}{RT} - \frac{\Delta H^0}{RT} \qquad (15)$$

Here, Ke represents the equilibrium constant, qe presents the adsorption capacity (mg/g), C_e is the concentration of dye at equilibrium, R and T represent the gas constant (8.314 J/K mol), and temperature in kelvin (K), respectively.

The calculated values are presented in Table 3, and a plot of ln K vs1/T and a plot of temperature impact on adsorption capacity are presented in Figure 13, showing the linear plot of ln K_e vs ln 1/T, confirming the applicability of the van't Hoff equation. It was noticed that the rate of adsorption is increasing with an increase in temperature. Kumar and group have shown a similar data trend (Yadav et al., 2024a). It can be explained by the fact that as temperature increases, there is an increase in entropy, leading to an increase in the kinetic energy of adsorbate molecules. Also, as the temperature rises, adsorbate molecules in the solution become more mobile, leading to more collisions with the adsorbent's active sites. The positive enthalpy change, ΔH^0 = 22.40 kJ/mol, confirms the endothermic nature of the adsorption process. Additionally, the negative Gibbs free energy values (ΔG^0 ranging from -1.589 to -1.777 kJ/mol) at the studied temperatures indicate the spontaneity of the adsorption. The increase in adsorption capacity with

temperature can be attributed to enhanced kinetic energy and mobility of dye molecules, leading to more frequent collisions with the adsorbent's active sites. Moreover, the entropy change, ΔS^{o} = -100.25 J/mol^{-1}K, suggests increased randomness at the solid-liquid interface during adsorption (Pandey & Singh, 2023). In addition to that, activation energy and surface coverage have been calculated and found to be 22.398 KJ and 0.043, respectively.

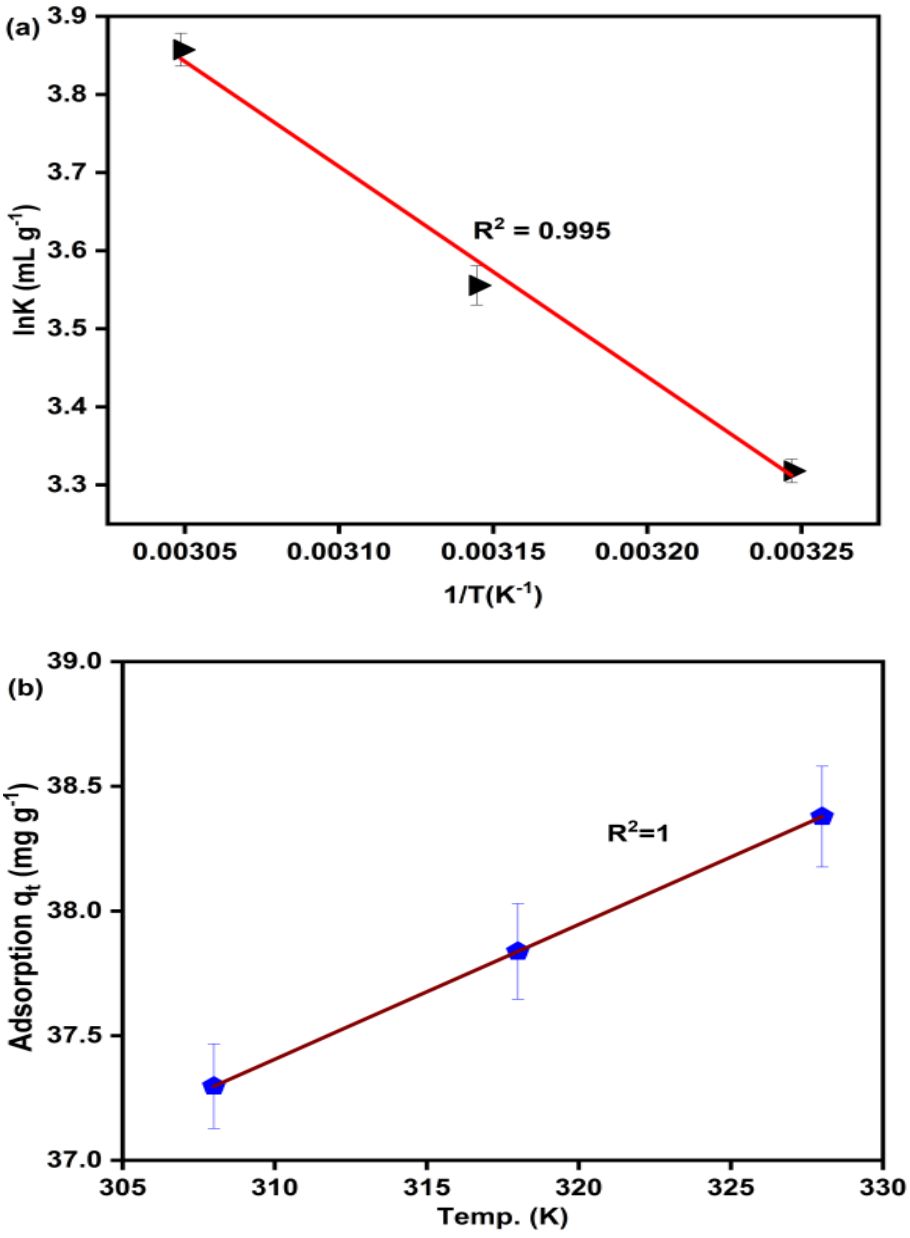

Figure 13. (a)Van't Hoff plot for ln K versus 1/T for CV, (b) effect of temperature on adsorption capacity for CV.

Table 3 Temperature-dependent parameters for CV uptake. The data presented by the mean ± standard deviation ($P < 0.05$)

Temperature (K)	Δ H (KJ mol^{-1})	Δ S^o (J $mol^{-1}K^{-1}$)	Δ G^o (KJ mol^{-1})
308.15	22.397	-100.25	-1.589
318.15			-1.684
328.15			-1.777

4.6 Binary mixture of dye

To check the potential of synthesized adsorbent in the dye removal efficacy of more complex systems, CV and MB dyes were added into the aqueous solution by maintaining the 1:1 ratio with a concentration of 20 mg L^{-1} of both dyes and 0.1 g adsorbent was added into it and subjected for shaking in an orbital shaker for 60 min at 100 rpm at ambient temperature. For the binary system, absorption maxima of CV and MB were recorded at 592 nm and 664 nm. It was observed that ACG has good removal efficiency towards CV (86 %) and MB (78 %) in binary systems represented in Figure 14a.

4.7 Regeneration and recyclability

To ensure the reproducibility of activated phytosorbent, the regeneration capability of the phytosorbent was checked for its practical importance. The batch experiments were conducted to perform the study. In order to regenerate the phytosorbent, the phytosorbent was collected and washed with 1 M HCl and 1 M NaOH solutions, which helped to regenerate binding sites. Further, the phytosorbent was washed with distilled water to remove excess HCl and NaOH. After washing the phytosorbent, it was dried at ambient temperatures and used in the next cycles. The same procedure was followed up to 4 cycles. It was observed that the % dye adsorption was found to be more than 88 % till 4 cycles, as presented in Figure 14b. This suggests that it can be reused and can be implemented to remediate polluted water.

4.8 Adsorption in Real wastewater samples

The adsorption capacity of the adsorbent was observed for CV dye sequestration in real industrial water samples. The real sample was collected from the Industrial Area, Badli, New Delhi. The dye concentration has been spiked in a sample containing dyes and other effluents. Thus, in order to observe the effect of CV, dyes of known concentration were added to the sample. Then, the adsorption was performed in real water sample and the obtained results were compared with distilled water, shown in Fig. 14c. Further, the percentage removal efficacy of dye in real sample was found to be 79.6 %. Thus, the synthesized material can be utilized in environmental remediation.

4.9 Impact of Ionic Strength

Figure 14d illustrates the effect of salt solution concentration on the dye removal efficiency using adsorbents in 0.05 N salt solutions of NaCl, $CaCl_2$, and $AlCl_3$. The adsorption experiments were carried out with 0.1 g of adsorbent. It was observed that as the ionic strength increases, removal efficacy decreases. Therefore, divalent and trivalent ions strongly influence the adsorptive removal of CV dye relative to monovalent ions, which is in agreement with the adsorbent affinity with high charge densities (Pandey et al., 2021).

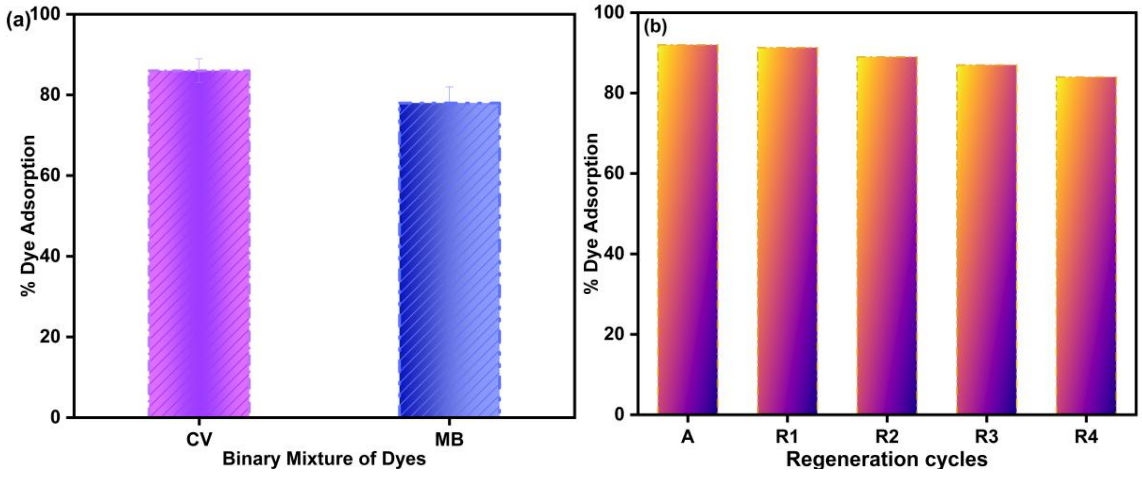

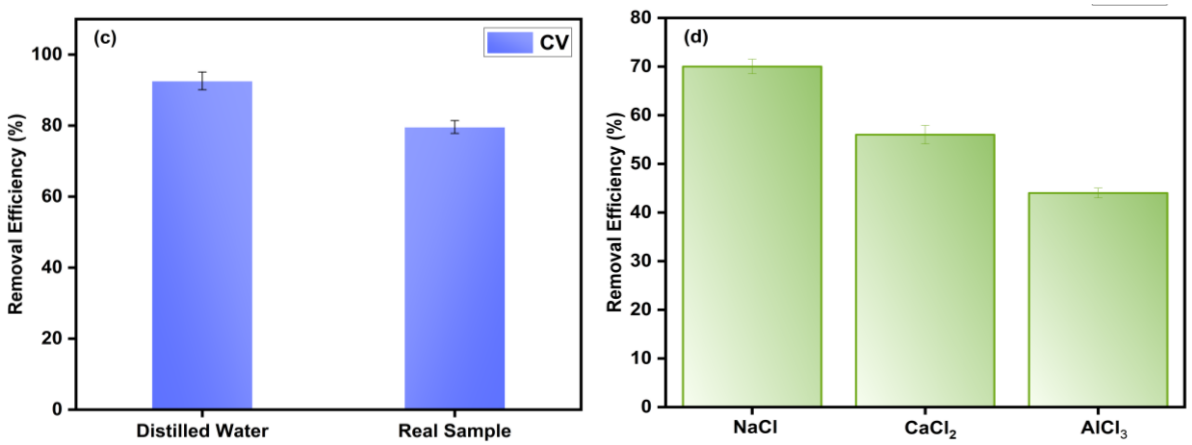

Figure 14. Plot of (a) simultaneous removal of CV and MB, (b) *regeneration cycles of phyto-sorbent for removal of CV, (c) Removal efficiency in real water sample, (d) effect of ions*

4.10 Probable Mechanism

An important fact to note is that the surface charge can modulate the dye adsorption. Accordingly, the present adsorption is associated with electrostatic attraction, weak van der Waals forces, and π-π stacking presented in Figure 15. Adsorption is higher above pH_{zpc} due to steric repulsion between cationic dye and negative surface charges (Bashir & Saleh, 2015; Dey et al., 2022). This explanation was supported by the DLS study, which shows that –ve charge on the adsorbent which helps to adsorb the CV dye on the sorbent surface.

Figure 15. Mechanism of Adsorption on the adsorbent

4.11 Different available adsorbent

This study also compared the removal efficiency and adsorption capacity of the synthesized adsorbent with some reported sorbents presented in Table 4. It was observed that our synthesized sorbent has better adsorption capacity compared with the reported adsorbents

Table 4. Different Adsorbents reported for the sequestration of dyes

S. No.	Adsorbent	% Removal	Adsorption Capacity	Ref.
1.	Zeolite/algae composite	78.9	11.26	(Dryaz et al., 2021)
2.	XG//PAM/Alginic acid	84	114.9	(G. Sharma et al., 2022)
3.	GG/*Ulva lactuca L.*/XG	92	62.83	(Kanwal et al., 2024)
4.	Cashew shell	98.5	5.18	(R. Sharma et al., 2016)
5.	GG/PAM	90	31	(Hiremath & Vishalakshi, 2015)
6.	Aminated avocado seed powder	14	47.2	(Munagapati et al., 2021)
7.	Chitosan@$Fe_2(MoO_4)_3$	90	69	(Pournamdari & Niknam, 2024)

8.	Activated *Calatropis Gigantea*	111.11	Present study

5. CONCLUSION

In this study, waste leaves of Calotropis Gigantea (CG), commonly known as Akh, an abundantly available but underutilized indigenous plant, were chemically modified using sodium hydroxide (NaOH) and utilized for the removal of crystal violet dye from aqueous solutions via the batch adsorption method. To the best of our knowledge, there are no prior reports available on the application of modified CG specifically for the sequestration of crystal violet. The modified CG demonstrated an impressive adsorption capacity of **111.11 mg/g**, which exceeds previously reported values available in the literature. The alkali activation process effectively removed lingo cellulosic barriers, enhancing porosity, surface area, and water stability, thereby making the material not only more efficient but also mechanically and chemically more stable than untreated biomass. This approach introduces a novel, eco-friendly, and scalable alternative to conventional and more expensive adsorbents, highlighting its potential for real-world wastewater treatment applications. The dried leaves utilized in this work are a biowaste obtained from the *Calotropis Gigantea* plant and were utilized as a phytosorbent for the sequestration of CV dye from aqueous media. The sorbent morphology was characterized using FESEM, shows fragmented and porous surface which supports the adsorption process. The impact of various parameters, including contact time, concentrations, and others, were performed, and it was found that **~92%** removal of CV dye from aqueous media in 1 hour. Further, isotherm and kinetic studies were performed, which revealed that sorbent follows monolayer adsorption and pseudo-second order. In addition to that, regeneration study was also performed and it was found out that the sorbent is efficiently adsorbed CV dye after 4 cycles. Hence, the sorbent can be used in practical importance.

REFERENCES

1. Ahmed, M., Mavukkandy, M. O., Giwa, A., Naddeo, V., & Hasan, S. W. (**2022**). Recent developments in hazardous pollutants removal from wastewater and water reuse within a circular economy. *Npj Clean Water*, 1–25. https://doi.org/10.1038/s41545-022-00154-5

2. Ajiboye, T. O., Oyewo, O. A., & Onwudiwe, D. C. (**2021**). Adsorption and photocatalytic removal of Rhodamine B from wastewater using carbon-based materials. *FlatChem*, *29*(August), 100277. https://doi.org/10.1016/j.flatc.2021.100277

3. Akl, Z. F., Zaki, E. G., & ElSaeed, S. M. (**2021**). Green Hydrogel-Biochar Composite for Enhanced Adsorption of Uranium. *ACS Omega*, *6*(50), 34193–34205. https://doi.org/10.1021/acsomega.1c01559

4. Akpomie, K. G., & Conradie, J. (**2023**). Efficient adsorptive removal of paracetamol and thiazolyl blue from polluted water onto biosynthesized copper oxide nanoparticles. *Scientific Reports*, *13*(1), 1–16. https://doi.org/10.1038/s41598-023-28122-0

5. Al-Asadi, S. T., Al-Qaim, F. F., Al-Saedi, H. F. S., Deyab, I. F., Kamyab, H., & Chelliapan, S. (**2023)**. Adsorption of methylene blue dye from aqueous solution using low-cost adsorbent: kinetic, isotherm adsorption, and thermodynamic studies. *Environmental Monitoring and Assessment*, *195*(6). https://doi.org/10.1007/s10661-023-11334-2

6. Ayawei, N., Ebelegi, A. N., & Wankasi, D. (**2017**). Modelling and Interpretation of Adsorption Isotherms. In *Journal of Chemistry* (Vol. 2017). https://doi.org/10.1155/2017/3039817

7. Bashir, A., & Saleh, B. (**2015**). *Powdered Beet Red Roots Using as Adsorbent to Removal of Methylene Blue Dye from Aqueous Solutions*. *December 2014*.

8. Belmabrouk, H., Brahem, R. A., Jabli, M., El-ghoul, Y., Alminderej, F. M., & Alharbi, T. (**2023**). Characterization of Raw and Treated Calotropis Gigantea Fibers : Application to

the Adsorption of Methylene Blue Dye Characterization of Raw and Treated Calotropis Gigantea Fibers : Application to the Adsorption of Methylene Blue Dye. *Journal of Natural Fibers*, *20*(1). https://doi.org/10.1080/15440478.2022.2160401

10. Bora, A., & Karak, N. (**2022)**. Starch and itaconic acid-based superabsorbent hydrogels for agricultural application. *European Polymer Journal*, *176*(July), 111430. https://doi.org/10.1016/j.eurpolymj.2022.111430
11. Bullen, J. C., Saleesongsom, S., Gallagher, K., & Weiss, D. J. (**2021**). A Revised Pseudo-Second-Order Kinetic Model for Adsorption, Sensitive to Changes in Adsorbate and Adsorbent Concentrations. *Langmuir*, *37*(10), 3189–3201. https://doi.org/10.1021/acs.langmuir.1c00142
12. Dey, S., Chakraborty, R., Mohanta, J., & Dey, B. (**2022**). Tricosanthes cucumerina: a potential biomass for efficient removal of methylene blue from water. *Bioremediation Journal*, *0*(0), 1–15. https://doi.org/10.1080/10889868.2022.2086530
13. Dimbo, D., Abewaa, M., Adino, E., Mengistu, A., Takele, T., Oro, A., & Rangaraju, M. (**2024**). Methylene blue adsorption from aqueous solution using activated carbon of spathodea campanulata. *Results in Engineering*, *21*(February), 101910. https://doi.org/10.1016/j.rineng.2024.101910
14. Doan Thi, T. U., Nguyen, T. T., Thi, Y. D., Ta Thi, K. H., Phan, B. T., & Pham, K. N. (**2020**). Green synthesis of ZnO nanoparticles using orange fruit peel extract for antibacterial activities. *RSC Advances*, *10*(40), 23899–23907. https://doi.org/10.1039/d0ra04926c
15. Dutta, S., Gupta, B., Srivastava, S. K., & Gupta, A. K. (**2021**). Recent advances on the removal of dyes from wastewater using various adsorbents: A critical review. *Materials Advances*, *2*(14), 4497–4531. https://doi.org/10.1039/d1ma00354b
16. Elgarahy, A. M., Elwakeel, K. Z., Mohammad, S. H., & Elshoubaky, G. A. (**2021**). A

critical review of biosorption of dyes, heavy metals and metalloids from wastewater as an efficient and green process. In *Cleaner Engineering and Technology* (Vol. 4, Issue November 2020, p. 100209). Elsevier Ltd. https://doi.org/10.1016/j.clet.2021.100209

17. Freundlich, H. **(1907)**. Über die Adsorption in Lösungen. *Zeitschrift Für Physikalische Chemie*, *57U*(1), 385–470. https://doi.org/10.1515/zpch-1907-5723

18. Ghoniem, M. G., Ali, F. A. M., Abdulkhair, B. Y., Elamin, M. R. A., Alqahtani, A. M., Rahali, S., & Ben Aissa, M. A. **(2022).** Highly Selective Removal of Cationic Dyes from Wastewater by MgO Nanorods. *Nanomaterials*, *12*(6), 1–14. https://doi.org/10.3390/nano12061023

19. Indu Rani, Sudhir Warkar, A. K. **(2024)**. *Silver Nanoparticle-Embedded Tamarind Kernel Gum Poly Sodium Acrylate Nanocomposite for Sustainable release of Doxycycline*. https://doi.org/doi.org/10.1002/slct.202400168 www.chemistryselect.org

20. Issabayeva, G., Wong, S. H., Pang, C. Y., Wong, M. C., & Aroua, M. K. **(2022)**. Fluoride removal by low-cost palm shell activated carbon modified with prawn shell chitosan adsorbents. *International Journal of Environmental Science and Technology*, *19*(5), 3731–3740. https://doi.org/10.1007/s13762-021-03448-2

21. Kalam, S., Abu-khamsin, S. A., Kamal, M. S., & Patil, S. **(2021)**. *Surfactant Adsorption Isotherms : A Review*. https://doi.org/10.1021/acsomega.1c04661

22. Kaur, R., & Kaur, H. (2017). Calotropis procera an effective adsorbent for removal of Congo red dye: isotherm and kinetics modelling. *Modeling Earth Systems and Environment*, *3*(1), 1–13. https://doi.org/10.1007/s40808-017-0274-3

23. Lellis, B., Fávaro-Polonio, C. Z., Pamphile, J. A., & Polonio, J. C. (**2019)**. Effects of textile dyes on health and the environment and bioremediation potential of living organisms. *Biotechnology Research and Innovation*, *3*(2), 275–290. https://doi.org/10.1016/j.biori.2019.09.001

24. Mahato, R., Qaiyum, M. A., Samal, P. P., Dutta, S., Dey, B., & Dey, S. **(2022)**. Exploring the promising potential of fallen bamboo leaves (Bambusa bambos) for efficient removal of crystal violet from wastewater . *International Journal of Phytoremediation*, *0*(0), 1–10. https://doi.org/10.1080/15226514.2022.2125498

25. Mohanta, J., Kumari, R., Qaiyum, M. A., Dey, B., & Dey, S. **(2021).** Alkali assisted hydrophobic reinforcement of coconut fiber for enhanced removal of cationic dyes: equilibrium, kinetics, and thermodynamic insight. *International Journal of Phytoremediation*, *23*(13), 1423–1431. https://doi.org/10.1080/15226514.2021.1901850

26. Mori, A., & Maksimov, I. L. **(1999)**. On the Temkin model of solid-liquid interface. *Journal of Crystal Growth*, *200*(1–2), 297–304. https://doi.org/10.1016/S0022-0248(98)01397-9

27. Musah, M., Azeh, Y., Mathew, J., Umar, M., Abdulhamid, Z., & Muhammad, A. (**2022)**. Adsorption Kinetics and Isotherm Models: A Review. *Caliphate Journal of Science and Technology*, *4*(1), 20–26. https://doi.org/10.4314/cajost.v4i1.3

28. Musie, W., & Gonfa, G. **(2023).** Fresh water resource, scarcity, water salinity challenges and possible remedies: A review. *Heliyon*, *9*(8), e18685. https://doi.org/10.1016/j.heliyon.2023.e18685

29. Pandey, B., & Singh, P. **(2023)**. Statistical Optimization of Process Parameters for Ultrafast Uptake of Anionic Azo Dyes by Efficient Sorbent: Zn/Cu Layered Double Hydroxide. *Applied Organometallic Chemistry*, *March*, 1–18. https://doi.org/10.1002/aoc.7072

30. Pathak, J., & Singh, P. **(2023**a). Adsorptive Removal of Congo Red Using Organically Modified Zinc–Copper–Nickel Ternary Metal Hydroxide: Kinetics, Isotherms and Adsorption Studies. *Journal of Polymers and the Environment*, *31*(1), 327–344. https://doi.org/10.1007/s10924-022-02612-0

31. Pathak, J., & Singh, P. **(2023b)**. Adsorptive Removal of Congo Red Using Organically Modified Zinc–Copper–Nickel Ternary Metal Hydroxide: Kinetics, Isotherms and Adsorption Studies. *Journal of Polymers and the Environment*, *31*(1), 327–344. https://doi.org/10.1007/s10924-022-02612-0

32. Qaiyum, M. A., Mohanta, J., Kumari, R., Samal, P. P., Dey, B., & Dey, S. **(2022)**. Alkali treated water chestnut (Trapa natans L.) shells as a promising phytosorbent for malachite green removal from water. *International Journal of Phytoremediation*, *24*(8), 822–830. https://doi.org/10.1080/15226514.2021.1977912

33. Qaiyum, M. A., Sahu, P. R., Samal, P. P., Dutta, S., Dey, B., & Dey, S. **(2022)**. Towards a win-win chemistry: extraction of C.I. orange from Kamala fruit (Mallotus philippensis), and simultaneous exercise of its peels for the removal of Methylene Blue from water. *International Journal of Phytoremediation*, *0*(0), 1–10. https://doi.org/10.1080/15226514.2022.2119936

34. Quansah, J. O., Hlaing, T., Lyonga, F. N., Kyi, P. P., Hong, S. H., Lee, C. G., & Park, S. J. **(2020).** Nascent rice husk as an adsorbent for removing cationic dyes from textile wastewater. *Applied Sciences (Switzerland)*, *10*(10). https://doi.org/10.3390/app10103437

35. Rani, K. C., Naik, A., Chaurasiya, R. S., & Raghavarao, K. S. M. S. **(2017)**. Removal of toxic Congo red dye from water employing low-cost coconut residual fiber. *Water Science and Technology*, *75*(9), 2225–2236. https://doi.org/10.2166/wst.2017.109

36. Rout, A., Qaiyum, M. A., Samal, P. P., Dutta, S., Dey, B., & Dey, S. **(2022)**. Brinjal (Solanum melongena) stalk waste as an effective scavenger for Eriochrome Black-T from water and wastewater: an approach towards waste to best . *International Journal of Phytoremediation*, *0*(0), 1–9. https://doi.org/10.1080/15226514.2022.2123445

37. Shanaah, H. H., Alzaimoor, E. F. H., Rashdan, S., & Abdalhafith, A. A. **(2023).**

Photocatalytic Degradation and Adsorptive Removal of Emerging Organic Pesticides Using Metal Oxide and Their Composites : Recent Trends and Future Perspectives.

38. Sun, Z., Wang, L., Jiang, X., Bai, L., Wang, W., Chen, H., Yang, L., Yang, H., & Wei, D. (**2020**). Self-healing, sensitive and antifreezing biomass nanocomposite hydrogels based on hydroxypropyl guar gum and application in flexible sensors. *International Journal of Biological Macromolecules*, *155*, 1569–1577. https://doi.org/10.1016/j.ijbiomac.2019.11.134

39. Tahir, N., Bhatti, H. N., Iqbal, M., & Noreen, S. (**2016)**. Bio-molecules composite with peanut hull waste and application for Crystal Violet adsorption. *International Journal of Biological Macromolecules*. https://doi.org/10.1016/j.ijbiomac.2016.10.013

40. Wu, F., Tseng, R., & Juang, R. (**2009**). *Characteristics of Elovich equation used for the analysis of adsorption kinetics in dye-chitosan systems*. *150*, 366–373. https://doi.org/10.1016/j.cej.2009.01.014

41. Yadav, P., Warkar, S. G., & Kumar, A. (**2024**a). Biopolymer-CMTG and m-BPDM Based Hydrogel Composite for Promising Sensing of Zinc, Cadmium, and Mercury in Aqueous Medium. *Journal of Inorganic and Organometallic Polymers and Materials*, *Cd*. https://doi.org/10.1007/s10904-024-03224-y

42. Yadav, P., Warkar, S. G., & Kumar, A. (**a**b). Development of graphene oxide-incorporated biopolymer-carboxymethyl tamarind kernel gum-based hydrogel as an effective adsorbent for the sequestration of dye pollutants. *Polymer Engineering and Science*, *64*(10), 1–18. https://doi.org/10.1002/pen.26883

43. Yahya, N. A., Abdul Wahab, R., Attan, N., Abdul Hamid, M., Mohamed Noor, N., & Kobun, R. (**2022**). Ananas comosus Peels Extract as a New Natural Cosmetic Ingredient: Oil-in-Water (O/W) Topical Nano Cream Stability and Safety Evaluation. *Evidence-Based Complementary and Alternative Medicine*, *2022*.

https://doi.org/10.1155/2022/2915644

44. Yusuff, A. S. (**2022**). *Adsorptive removal of lead and cadmium ions from aqueous solutions by aluminium oxide modified onion skin wastes : Adsorbent characterization , equilibrium modelling and kinetic studies*. https://doi.org/10.1177/0958305X21989886